Journal of Materials Chemistry A

Accepted Manuscript

ROYAL SOCIETY OF CHEMISTRY

www.rsc.org/materialsA

Journal Name

RSCPublishing

COMMUNICATION

Enhancing photocurrent of perovskite solar cells via modification of $TiO_2/CH_3NH_3PbI_3$ heterojunction interface with amino acid

Cite this: DOI: 10.1039/x0xx00000x

Y. C. Shih,[a] L. Y. Wang,*[b,c] H. C. Hsieh,[a] and K. F. Lin*[a,b]

Received ooth January 2012,
Accepted ooth January 2012

DOI: 10.1039/x0xx00000x

www.rsc.org/

In this communication, glycine, an amino acid, was applied to modify the $TiO_2/CH_3NH_3PbI_3$ heterojunction interface for reducing the inevitable defects formed during crystallization of perovskite. The power conversion efficiency of resulting perovskite solar cell was increased from 8.35 to 12.02%, attributed to the enhancement of short-circuit current density.

Since the pioneering work at 2009, organolead halide perovskites ($CH_3NH_3PbX_3$, X=Cl, Br, I) have evolved as a promising light sensitizer for the next generation of dye-sensitized solar cells[1], due to their superb light-harvesting characteristics and ambipolar transport property[2-4]. Within a short period of time, the configuration of devices from liquid type[1,5] to all solid type[6] was achieved by substituting the liquid electrolyte with hole transporting material such as 2,2',7,7'-tetrakis(N,N-di-p-methoxyphenylamine)-9,9-spirobifluorene (spiro-MeOTAD). Nowadays, perovskite solar cells can be divided into two categories: one is heterojunction (with mesoporous metal oxide) and the other is planar structure cells with a p-i-n junction, both exhibited the high power conversion efficiency (PCE) of 18.4%[7] and 19.3%[8], respectively.

Although planar perovskite solar cells showed the higher PCE and simpler manufacturing process, mesoporous metal oxide such as TiO_2 could prevent short circuiting between working and counter electrodes[9]. In addition, the porous TiO_2 (p-TiO_2) layer may plays as a scaffold to elongate the optical light path and retard the charge recombination[10]. However, the incomplete pore-filling of TiO_2 with perovskite to decline the performance of devices was the major concern with this process[11]. Hence two-step deposition by spin-coating PbI_2 on top of the p-TiO_2 layer and then crystallizing with CH_3NH_3I to fabricate the perovskite light harvester was developed to reduce the morphological variation of perovskite[12]. Notably, although the photovoltaic performance and reproducibility of the solar cells were improved, the deposition of perovskite crystals on the TiO_2 scaffold still inevitably caused defects at the $TiO_2/CH_3NH_3PbI_3$ heterojunction. Recently, several research groups reported that the photovoltaic performance of perovskite solar cells could be improved through amphipathic molecule treatment on TiO_2 surface[13-15]. Therefore, in this work, we modified the $TiO_2/CH_3NH_3PbI_3$ interface by introducing glycine, a kind of amino acid, as a coupling agent. Through this modification, the best PCE of perovskite solar cell was increased from 8.35 to 12.02%, mainly due to the enhancement of short-circuit current density (J_{sc}) from 14.42 to 19.54 mA cm^{-2}.

Photovoltaic characterization of solar cells was carried out at full sunlight (100 mW cm^{-2}) with a 1000 W ozone-free Xenon lamp equipped with a water-based IR filter and AM 1.5 filter (Newport Corporation). Measured condition was set as forward scan (from forward bias to short-circuit) with a scan rate of 0.1 V s^{-1}. Fig. 1 shows the best *J-V* curves of perovskite solar cells based on the TiO_2 treated with and without glycine.

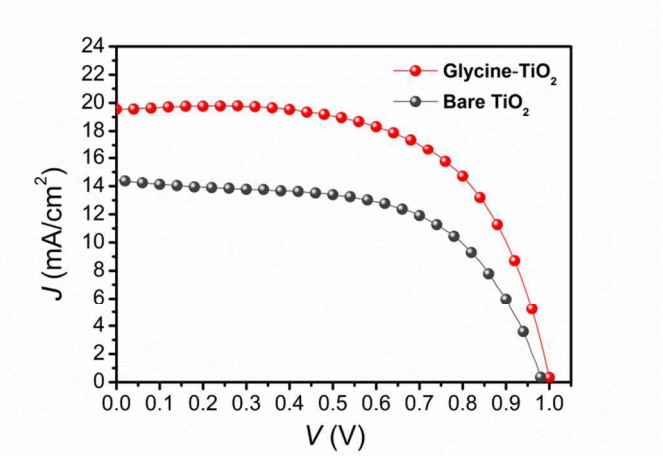

Fig. 1 *J–V* curves of the best perovskite solar cells with bare TiO_2 (dark gray curve) and glycine-treated TiO_2 (red curve).

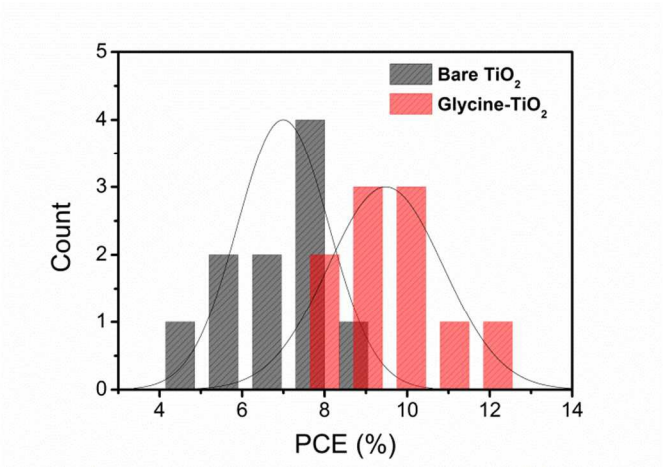

Fig. 2 Histograms of photovoltaic PCEs. Data were collected from 10 perovskite solar cells based on TiO_2 with (red) or without (dark gray) glycine treatment.

Table 1 Photovoltaic performance data of the perovskite solar cells with and without modification of glycine.

Sample	J_{SC} (mA cm^{-2})	V_{OC} (V)	*FF*	PCE (%)
Bare TiO_2	12.56±1.70	0.95±0.02	0.58±0.04	6.99±1.11
Glycine-TiO_2	16.20±2.31	0.98±0.02	0.60±0.05	9.48±1.40

Obviously the glycine modified sample exhibited much higher photocurrent than the non-modified one. Fig. 2 shows the statistical PCE values on a larger batch of ten photovoltaic devices. All the average parameters with glycine-treated TiO_2 were superior to those with bare TiO_2 as can be seen in Table 1. The average PCE of perovskite solar cells was increased from 6.99 to 9.48%, mainly due to the improvement of J_{sc} since the open-circuit voltage (V_{oc}) and fill factor (*FF*) were barely enhanced. X-ray diffraction (XRD, PANalytical X'Pert PRO) was conducted to analyze the crystallography of perovskite with a scan step size of 0.013° and 3.57 s for each step (Fig. S1). The appearance of diffraction peaks were agreed with the published literatures[12,16]. However, unfortunately, it is hard to compare the results of the perovskite deposited on mesoporous TiO_2 with and without treatment of glycine. It might be due to the fact that the tiny amount of perovskite crystals formed in the interface of TiO_2/$CH_3NH_3PbI_3$ was barely detected by X-ray diffraction.

Therefore, to realize how the amino acid affected the crystallization of PbI_2, we investigated the crystal structure of PbI_2 on top of the compact TiO_2 (c-TiO_2) with and without glycine treatment in a planar configuration first. Fig. 3(a) shows their XRD patterns. The crystal of PbI_2 is a layered structure with the basic building block that Pb atoms are sandwiched in between two layers of I atoms[17]. In Fig. 3(a), the diffraction peaks of PbI_2 can be indexed as a hexagonal system (JCPDS, PDF number 07-0235), the (001) lattice plane is clearly observed for both samples. However, the sample treated with glycine exhibited stronger signals at (002), (003), and (004) lattice planes, implying the PbI_2 tended to grow in an orientation along the *c* axis. As can been seen in scanning electron microscope (SEM, JEOL JSM-6300) images, the morphology of PbI_2 depositing on glycine-treated c-TiO_2 (Fig. 4(a)) differ from the bare c-TiO_2 (Fig. 4(b)). Without glycine, PbI_2 crystallized into a broader size range of 200-600 nm with more voids. In contrast, the PbI_2 grown on the glycine-treated c-TiO_2 displays less and smaller voids with narrow crystal size range of 200-300 nm. Obviously, glycine has induced PbI_2 crystals to grow along the *c* axis with the direction perpendicular to the TiO_2 surface, beneficial to the following perovskite crystallization.

Fig. 3(b) shows the XRD patterns of $CH_3NH_3PbI_3$ perovskite prepared by using the previous PbI_2 to crystallize with CH_3NH_3I (see ESI† for experimental details). Compared to the bare c-TiO_2, the treatment of glycine rendered the perovskite to appear stronger diffractions at (111) and (404) lattice planes. However, we did not observe any apparent difference between these two perovskites in the SEM investigation (see Fig. S2). It may be due to the fact that the usual information depth of XRD measurement ranging from a few micrometers to a few hundred

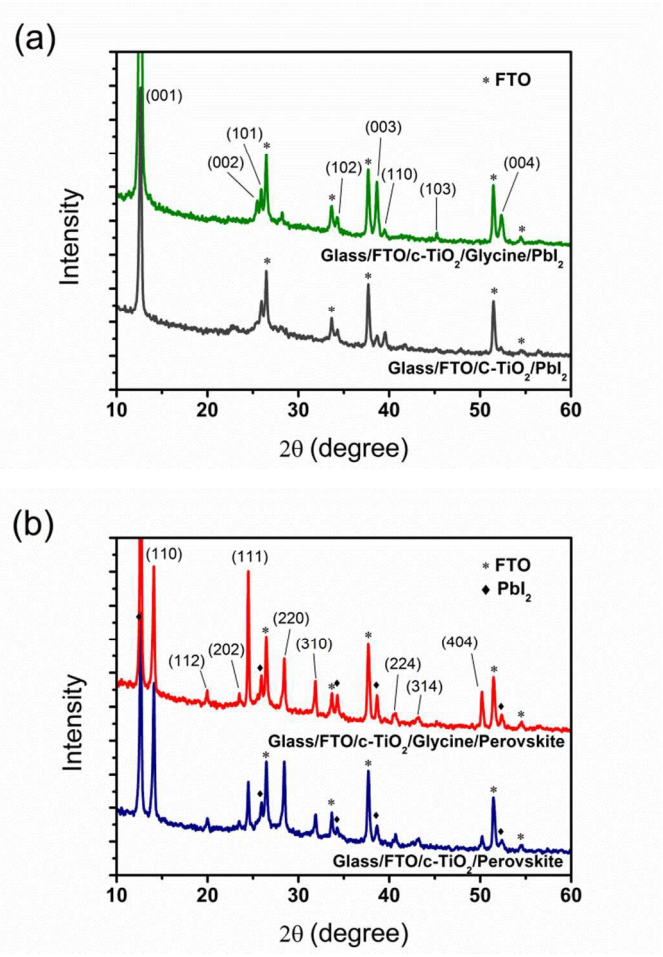

Fig. 3 XRD patterns of (a) PbI_2 and (b) $CH_3NH_3PbI_3$ formed on c-TiO_2 with and without glycine treatment.

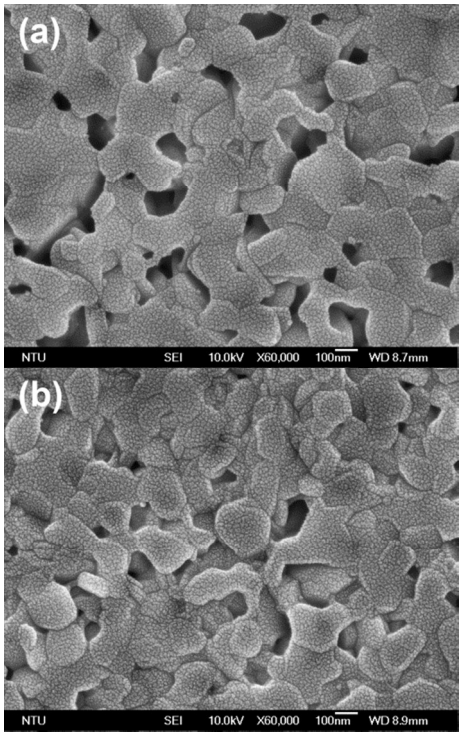

Fig. 4 SEM images of PbI_2 deposited on (a) bare c-TiO_2 and (b) glycine-treated c-TiO_2.

micrometers is deeper than the thickness of perovskite (~300 nm) and the subtle change of lattice plane induced by glycine was beneath the surface investigated by SEM. To further explore the crystal growth immediately on the surface of TiO_2, we diluted the original 1.0 M PbI_2 solution to ~0.1 M and investigate the surface morphology of resulting perovskite with SEM. Notably, the crystalline structure of PbI_2 immediately grew on the glycine-treated c-TiO_2 also shows less and smaller voids (see Fig. S3). As it was crystallized with CH_3NH_3I, the resulting $CH_3NH_3PbI_3$ perovskite crystals covering on the surface of TiO_2 was significantly more completed than that on non-modified TiO_2 (see Fig. 5), possibly owing to the denser PbI_2 crystals on the surface performing as the foundation for growth of the perovskite crystals.

Moreover, the growth of $CH_3NH_3PbI_3$ perovskite crystals on glycine-treated c-TiO_2 preferred their [111] direction which is consistent with the XRD Patterns (see Fig. 3b) and the size was also larger. Presumably, the carboxylic acid group of glycine was prone to anchor on the TiO_2, whereas its outward amine group acted as the nucleation center for PbI_2 deposition and crystal growth and herewith directly participated in the crystallization process of perovskite. The well-covered crystals on the TiO_2 surface observed in Fig. 5(b) support this proposed mechanism. By comparing the SEM images between Fig. S3(a) and Fig. 5(a), the $CH_3NH_3PbI_3$ perovskite crystals did not fully hold onto the top of bare c-TiO_2 during crystallization. In contrast, the glycine-treated surface was apt to keep the perovskite on the TiO_2 surface and promoted the crystal to grow evenly. This advanced the higher coverage of crystallized perovskite at the interface of $TiO_2/CH_3NH_3PbI_3$.

To further investigate the contribution of $TiO_2/CH_3NH_3PbI_3$ interface to the photovoltaic performance, electrochemical impedance spectroscopy (EIS) was employed to characterize the charge transfer dynamics of perovskite solar cells with a real configuration (containing p-TiO_2) by analysing the variation in impedance related to the different interfaces of the device[18-22]. As shown in Fig. 6, Nyquist plots of the perovskite solar cells based on bare TiO_2 and glycine-treated TiO_2 analysed under illumination were fitted well with Z-view software by setting the equivalent circuit shown in the inset figure. Three R-C circuits in series were employed. (Note: We did not observe the feature contributed by the interface of spiro-MeOTAD/gold counter electrode at high frequency mentioned in ref. 15, probably due to the limited frequency range of our instrument.) In our case, the difference between two specimens was only the presence of glycine. The first arc in Fig. 6 shows the huge difference between the perovskite solar cells with and without modification of glycine. This result points out the strong influence of the $TiO_2/CH_3NH_3PbI_3$ interface upon the feature of the first arc. Similar result has also been reported in the literature[20]. Accordingly, in our system, the first arc combines the complex interfaces of $TiO_2/CH_3NH_3PbI_3$/spiro-MeOTAD. The reduced resistance at the first arc of glycine-modified device (from 213.6 Ω to 101.8 Ω) would be due to the better contact and coverage of perovskite on the TiO_2 surface. Besides, we also observed the transmission line following the first arc at intermediate frequency. The appearance of transmission line has been suggested to be due to the transport resistance of charges lower than the recombination resistance at the interface[21,23]. Therefore, the much lower resistance (reduced from 230.4 Ω to 44.8 Ω) at this region means the modification of $TiO_2/CH_3NH_3PbI_3$ heterojunction with glycine leaded to the more efficient charge transfer from perovskite to TiO_2. However, the feature of the second arc in Fig. 6 did not have much difference after modification of glycine (139.3 Ω for bare TiO_2 and 109.2 Ω for glycine-TiO_2). After all, the reduced

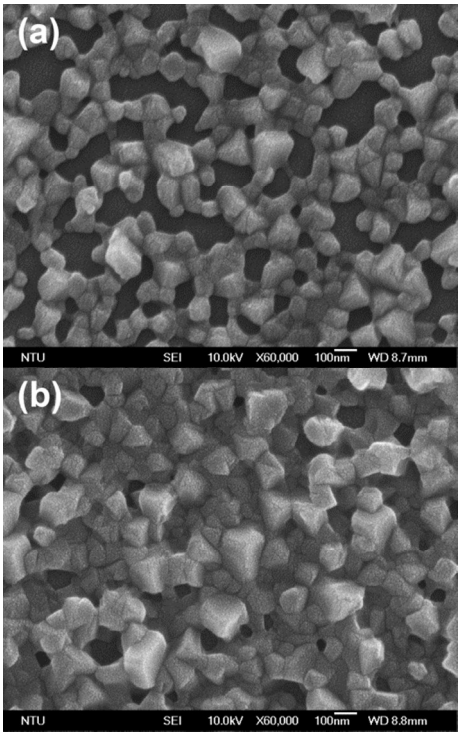

Fig. 5 SEM images of $CH_3NH_3PbI_3$ formed on (a) bare c-TiO_2 and (b) glycine-treated c-TiO_2. The $CH_3NH_3PbI_3$ was prepared through two-step deposition with pre-coated PbI_2 film using ~0.1M PbI_2 in DMF solution.

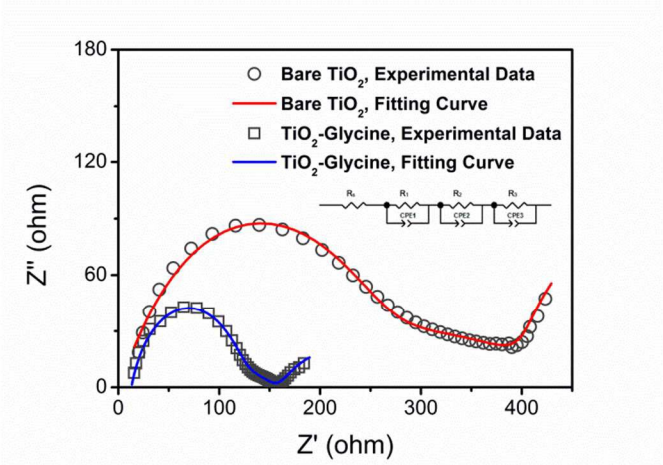

Fig. 6 Nyquist plots of perovskite solar cells based on bare TiO_2 (symbol ○) and glycine-treated TiO_2 (symbol □). Symbols are experimental data and solid lines correspond to the fitting results using the equivalent circuit shown in the inset figure. EIS were recorded with a potentiostat/galvanostat instrument (PGSTAT 302N, Autolab) equipped with FRA2 module under constant light illumination of 100 mW cm^{-2}. A DC applied bias voltage was set at open-circuit voltage of the perovskite solar cells with sinusoidal ac potential perturbation of 15 mV over a frequency range from 1 MHz to 0.01 Hz.

resistance by the modification of $TiO_2/CH_3NH_3PbI_3$ heterojunction with glycine was considered to be the major contribution to the better photovoltaic performance for perovskite solar cells.

Conclusions

We have successfully demonstrated the crucial role of amino acid as a coupling agent to modify the $TiO_2/CH_3NH_3PbI_3$ heterojunction interface for enhancing photovoltaic performance of two-step solution-processed perovskite solar cells. With this promising glycine modification, higher coverage of the $CH_3NH_3PbI_3$ crystals on TiO_2 surface was obtained, resulting in more efficient charge transfer and higher photocurrent. Based on our results, we believe that this modification has created a new breakthrough for the research of perovskite solar cells.

Acknowledgements

The authors acknowledge the financial support of the National Science Council in Taiwan, Republic of China, through grant NSC 103-2221-E-002-280-MY3, and Ministry of Science and Technology of the Republic of China through grant MOST 104-3113-E-002-010. This research was also supported by Academia Sinica through grant AS-103-SS-A02; 2394-104-0500.

Notes and references

[a] *Department of Materials Science and Engineering, National Taiwan University, Taipei, Taiwan.*
[b] *Institute of Polymer Science and Engineering, National Taiwan University, Taipei, Taiwan.*
[c] *Center for Condensed Matter Sciences, National Taiwan University, Taipei, Taiwan.*
[*] *Corresponding authors:*
Professor Leeyih Wang: E-mail: leewang@ntu.edu.tw;
Professor King-Fu Lin: Tel: +886-2-3366-1315; Fax: +886-2-2363-4562; E-mail: kflin@ntu.edu.tw;

†Electronic Supplementary Information (ESI) available: Experimental details, supporting XRD results and SEM images are included. See DOI: 10.1039/c000000x/

1. A. Kojima, K. Teshima, Y. Shirai and T. Miyasaka, *J. Am. Chem. Soc.*, 2009, **131**, 6050.
2. N.-G. Park, *J. Phys. Chem. Lett.*, 2013, **4**, 2423.
3. M. He, D. Zheng, M. Wang, C. Lin and Z. Lin, *J. Mater. Chem. A*, 2014, **2**, 5994.
4. H.-S. Kim, S. H. Im and N.-G. Park, *J. Phys. Chem. C*, 2014, **118**, 5615.
5. J.-H. Im, C.-R. Lee, J.-W. Lee, S.-W. Park and N.-G. Park, *Nanoscale*, 2011, **3**, 4088.
6. H.-S. Kim, C.-R. Lee, J.-H. Im, K.-B. Lee, T. Moehl, A. Marchioro, S.-J. Moon, R. Humphry-Baker, J.-H. Yum, J. E. Moser, M. Gratzel and N.-G. Park, *Sci. Rep.*, 2012, **2**, 591.
7. N. J. Jeon, J. H. Noh, W. S. Yang, Y. C. Kim, S. Ryu, J. Seo and S. I. Seok, *Nature*, 2015, **517**, 476.
8. H. Zhou, Q. Chen, G. Li, S. Luo, T.-b. Song, H.-S. Duan, Z. Hong, J. You, Y. Liu and Y. Yang, *Science*, 2014, **345**, 542.
9. G. Murugadoss, G. Mizuta, S. Tanaka, H. Nishino, T. Umeyama, H. Imahori and S. Ito, *APL Mater.*, 2014, **2**, 081511.
10. J.-W. Lee, T.-Y. Lee, P. J. Yoo, M. Gratzel, S. Mhaisalkar and N.-G. Park, *J. Mater. Chem. A*, 2014, **2**, 9251.
11. T. Leijtens, B. Lauber, G. E. Eperon, S. D. Stranks and H. J. Snaith, *J. Phys. Chem. Lett.*, 2014, **5**, 1096.
12. J. Burschka, N. Pellet, S.-J. Moon, R. Humphry-Baker, P. Gao, M. K. Nazeeruddin and M. Gratzel, *Nature*, 2013, **499**, 316.
13. Y. Ogomi, A. Morita, S. Tsukamoto, T. Saitho, Q. Shen, T. Toyoda, K. Yoshino, S. S. Pandey, T. Ma and S. Hayase, *J. Phys. Chem. C*, 2014, **118**, 16651.
14. A. Mei, X. Li, L. Liu, Z. Ku, T. Liu, Y. Rong, M. Xu, M. Hu, J. Chen, Y. Yang, M. Grätzel and H. Han, *Science*, 2014, **345**, 295.
15. L. Zuo, Z. Gu, T. Ye, W. Fu, G. Wu, H. Li and H. Chen, *J. Am. Chem. Soc.*, 2015, **137**, 2674.
16. Z. Ku, Y. Rong, M. Xu, T. Liu and H. Han, *Sci. Rep.*, 2013, **3**, 3132.
17. P. A. Beckmann, *Cryst. Res. Technol.*, 2010, **45**, 455.
18. H.-S. Kim, I. Mora-Sero, V. Gonzalez-Pedro, F. Fabregat-Santiago, E. J. Juarez-Perez, N.-G. Park and J. Bisquert, *Nat. Commun.*, 2013, **4**, 2242.
19. A. Dualeh, T. Moehl, N. Tétreault, J. Teuscher, P. Gao, M. K. Nazeeruddin and M. Grätzel, *ACS Nano*, 2013, **8**, 362.
20. E. J. Juarez-Perez, M. Wuβler, F. Fabregat-Santiago, K. Lakus-Wollny, E. Mankel, T. Mayer, W. Jaegermann and I. Mora-Sero, *J. Phys. Chem. Lett.*, 2014, **5**, 680.
21. V. Gonzalez-Pedro, E. J. Juarez-Perez, W.-S. Arsyad, E. M. Barea, F. Fabregat-Santiago, I. Mora-Sero and J. Bisquert, *Nano Lett.*, 2014, **14**, 888.
22. M. Yang, R. Guo, K. Kadel, Y. Liu, K. O'Shea, R. Bone, X. Wang, J. He and W. Li, *J. Mater. Chem. A*, 2014, **2**, 19616.

23. J. Bisquert, I. Mora-Sero and F. Fabregat-Santiago, *ChemElectroChem*, 2014, **1**, 289.

Table of contents

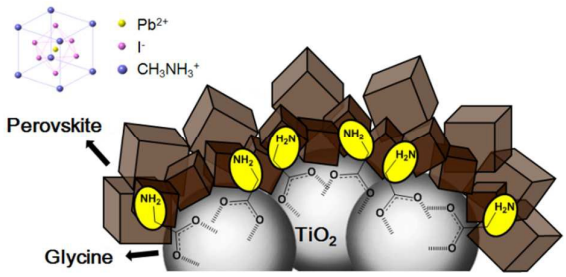

Novel modification of $TiO_2/CH_3NH_3PbI_3$ interface using glycine as a coupling agent induced higher coverage of perovskite through two-step solution process.